EIGENFREQUENCIES OF PERFORATED PLATES IN MEMS TRANSDUCERS: AN ANALYTICAL APPROXIMATION

Aneta Furmanová[1], Petr Honzík[1], Viktor Hruška[1], Pierrick Lotton[2]

[1] *Czech Technical University in Prague, Faculty of Electrical Engineering, Technicka 2, 166 27 Prague, Czech Republic*

[2] *Laboratoire d'Acoustique de l'Universite du Mans (LAUM), UMR 6613, Institut d'Acoustique - Graduate School (IA-GS), CNRS, Le Mans Universite, France*

This paper is a revised version of the authors' submitted manuscript that was peer-reviewed by at least two anonymous reviewers.

Abstract

Modern MEMS transducers frequently employ electrostatic transduction with perforated plates. Despite the prevalence of these devices, 3D numerical simulations of their structural vibrations remain computationally expensive, and a clear analytical understanding of the underlying physics is often lacking. This paper addresses these challenges by providing analytical approximations for the eigenfrequencies of clamped non-perforated and perforated square plates.

Using symbolic regression, we provide analytical approximations while avoiding the instabilities associated with high-degree polynomials. For perforated plates, the eigenfrequency is modeled as a normalized discrepancy to the solid case using a rational function characterized by only two geometry-dependent parameters. This sparse, interpretable form facilitates the subsequent derivation of the effective Young's modulus E^* and effective plate density ρ^*. To the best of our knowledge, this is the first work to employ symbolic regression for the analytical approximation of perforated plate eigenfrequencies.

Keywords: *electroacoustic transducers, perforated plate, symbolic regression*

1. Introduction

Most modern MEMS transducers utilize electrostatic transduction [1], featuring moving electrodes and perforated backplates in single [2] or double [3] configurations. There are two main reasons why one strives for analytical solutions or at least approximations when modelling the vibrational behaviour of these plates: numerical solvers are in 3D rather computationally expensive (even when employing symmetries), but first and foremost, we want to understand the underlying physical principles.

Šimonová *et al.* [4] have presented a theoretical model for the coupling between the acoustic field and the vibration of square perforated moving electrodes clamped at all boundaries. Building on this foundation, the present paper focuses on finding an analytical approximation for the eigenfrequencies of the moving electrode structural vibrations.

In our case, the eigenfrequency for the perforated plates can be provided as a discrepancy to the non-perforated case. For that, the normalized eigenfrequency was used, defined as the eigenfrequency of the perforated plate divided by the corresponding eigenfrequency of the non-perforated plate. Deepak *et al.* [5] describe normalized resonance frequency of perforated plates with a quartic polynomial. However, higher degree polynomials are not an optimal choice for regression, as they are unstable and prone to overfitting. A better choice is symbolic regression, which searches the space of mathematical expressions to identify a model that optimally represents the relationship between the predictors and the dependent variable [6]. To the best of our knowledge, we present here the first work employing symbolic regression for analytical approximation of the eigenfrequencies of perforated plates.

2. Theory

Analytical formulae for the eigenfrequencies are easily obtainable for membranes and simply supported plates. The eigenfrequency f_{mn} of a simply supported plate is given by the analytical expression:

$$f_{mn} = \frac{\pi}{2}\left(\frac{m^2}{a^2}+\frac{n^2}{b^2}\right)\sqrt{\frac{D}{\rho h}}\ , \tag{1}$$

where a and b are the plate's sides, h its thickness, ρ its density, and where $D = Eh^3/12(1-\nu^2)$ is the

Corresponding author: *furmaane@fel.cvut.cz.*

flexural rigidity, with E being the Young's modulus and ν the Poisson's ratio.
For fully clamped plates, an additional boundary condition (BC) must be satisfied: beyond the zero-displacement requirement (which applies to simply supported edges), the slope of the displacement must be equal to zero as well. Technically, both the homogeneous Dirichlet and Neumann BC must be satisfied at once. With these constraints, it becomes challenging to find exact analytical solutions that satisfy the governing equation and all the BCs [7].
Consequently, obtaining the eigenfrequencies for fully clamped plates relies on numerical simulations or approximation methods, such as the Rayleigh-Ritz method (see [8]) or analytical approaches based on series expansions (see, e.g. [9]). Therefore, the aim of this work is to provide an analytical approximation of the eigenfrequencies based on symbolic regression.

3. Non-perforated plates

To find the eigenfrequency approximation for non-perforated square plates clamped on all sides, symbolic regression with enforced prior knowledge was used. Namely, for the implementation, the open-source library PySR [10] was employed.
First, eigenfrequencies are calculated using COMSOL for different plate configurations defined by a set of given parameters: Young's modulus E, Poisson's ratio ν, material density ρ, and geometric parameters: the plate's side $2a$ and thickness h. For simplicity, only one material is considered in this paper, silicon.
The dataset was generated using the Solid Mechanics in COMSOL Multiphysics 6.4. The material properties used in COMSOL are displayed in Table 1.
A parametric sweep was employed for the geometry parameters in the following ranges: $a \in \{300, 600, 900, 1200, 1500\}$ μm, $h \in \{4, 7, 10, 13, 16\}$ μm. In total, 25 combinations of a, h were generated with modes $m, n = 1, 2, 3$, see the modes in Figure 1. Note the symmetries, which are due to the geometric symmetry of the square plate.
Symbolic regression is then used to determine the analytical expressions for the eigenfrequencies, yielding values as close as possible to those obtained by finite element analysis. Prior knowledge of the problem can be incorporated into the algorithm's setup. Based on the expressions for eigenfrequency of membranes (see, e.g. [11]) and simply supported plates (see, e.g. [8]), the following operators can be expected in the sought expression: `+,-,*,/,^`. Note that we can theoretically include all possible operators (e.g. trigonometric functions), but by doing so, the search space could

Parameter	Value	Unit
Young's modulus E	170	GPa
Poisson's ratio ν	0.28	1
Plate density ρ	2329	kg m^{-3}

Table 1: Material properties of the plate (silicon).

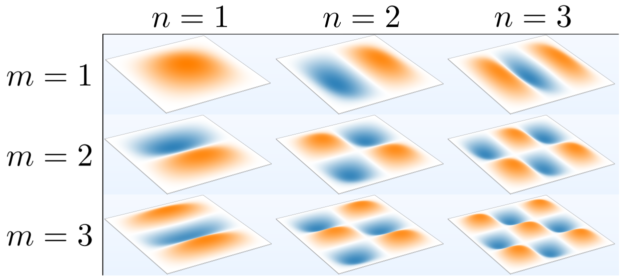

Figure 1: Eigenmodes of a non-perforated square plate.

grow exponentially. Moreover, the symmetry in m, n is expected due to the square geometry. Therefore, additional penalization for expressions not symmetric in m, n was added.
To optimize the regression process, several layers of expert knowledge were incorporated to refine the search space and improve the physical interpretability of the results. Based on the knowledge for the simply supported plate mode (Eq. (1)) and dimensional analysis, the formula can be expected in the following form

$$f_{mn} \propto \frac{1}{a^2}\sqrt{\frac{D}{\rho h}} = \frac{1}{a^2}\sqrt{\frac{Eh^2}{12(1-\nu^2)\rho}} \,, \tag{2}$$

when substituting for D. To restrict the search space a bit less, we remove the explicit h and a terms from the prefactor:

$$f_{mn} \propto \frac{1}{a}\sqrt{\frac{E}{12(1-\nu^2)\rho}} \,. \tag{3}$$

Rather than fitting the frequencies directly, we search for f_{mn}^2, as this quadratic form is more likely to lead to patterns similar to those found in literature. To ensure physical consistency, both the target and the candidate terms were cast into dimensionless forms:

$$(f_{mn} \cdot a)^2 \frac{12(1-\nu^2)\rho}{E} = g\left(\frac{h}{a}, m, n\right) \,, \tag{4}$$

The objective was set to minimize the L1 distance between the data and the predicted adjusted eigenfrequency. The mode numbers m and n were included as naturally dimensionless variables. Regarding the geometric parameters, the thickness-to-width ratio h/a was utilized as the primary feature, as this ratio is expected to play a role in the plate's vibrational response.

3.1. Results

Symbolic regression provides a Pareto front of candidate results, spanning from parsimonious but less accurate models to highly precise but complex ones that hinder interpretability. Selecting the optimal expression from this front is a trade-off between accuracy and interpretability.

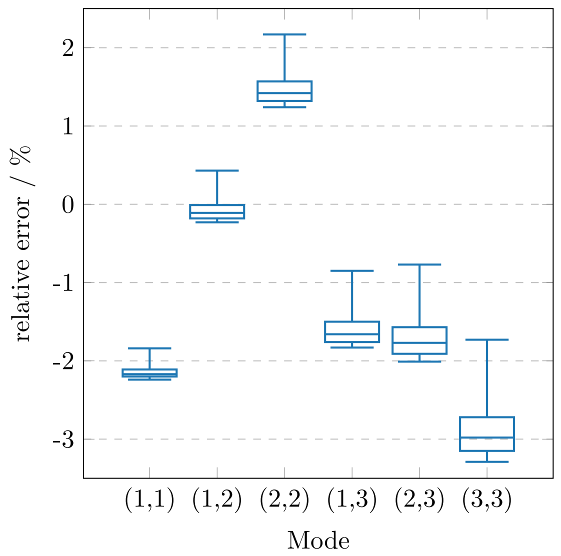

Figure 2: Eigenfrequency prediction error of Eq. (5)

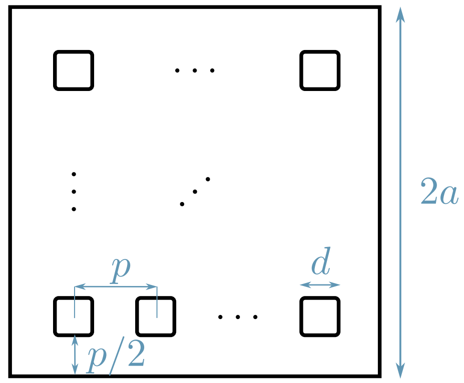

Figure 3: Schematic drawing of a square perforated plate.

The discovered formula reads

$$f_{mn} = \frac{0.201}{a^2}\sqrt{\frac{(m+n)^{5.6}}{(mn)^{1.16}}}\sqrt{\frac{Eh^2}{12(1-\nu^2)\rho}} \qquad (5)$$

The coefficient 0.201 in Eq. (5) was obtained by the least squares (`numpy.linalg.lstsq`). The relative error boxplots for different modes are shown in Figure 2. For the considered modes altogether, the median of the relative error is 1.71 %, first quartile 1.25 %, and the third quartile 2.17 %. These are lower errors than the interval widths provided by Leissa [8] (Tables 4.24–4.27), which are below 3 %.

4. Perforated plates

Building upon the non-perforated case, let's now consider the same square geometry with the introduction of a periodic array of perforations. The square perforated plate of thickness h and side $2a$ has now N square holes of side d and pitch p (see Figure 3). The number of holes is then equal to $N = 2a/p \times 2a/p$. The relative portion of perforations can be described in various ways; in this work, we utilize the following two criteria: the ligament efficiency η and the perforation ratio R. The ligament efficiency, defined as

$$\eta = \frac{p-d}{p}\ , \qquad (6)$$

represents the relative width of the material remaining between the holes. The perforation ratio

$$R = \frac{d^2}{p^2} \qquad (7)$$

describes the area-based density, representing the total area occupied by the holes relative to the total area of the plate.

In the following, the eigenfrequencies of the perforated plates are denoted f^* and we define the normalized eigenfrequency f^*/f where f is the eigenfrequency for the non-perforated plate.

Jhung *et al.* [12] suggest that the normalized eigenfrequency f^*/f does not depend on the mode number, but only on the relative portion of perforations. The authors demonstrate their findings for a single geometry with fixed a, h, and p and varying only d. To evaluate the applicability of these findings to perforated plates with MEMS transducers applications, this paper extends that study's findings to the micro-scale.

The independent variable of the function f^*/f can be either R or η, and since $R = (1-\eta)^2$, it is possible to easily switch from one to another. During a preliminary study, it turned out that having the perforation ratio R as an independent variable simplifies the shape of the normalized eigenfrequency function f^*/f and therefore makes it more suitable for regression. Therefore, the R was chosen to be regularly spaced as $R \in \{0.05, 0.10, \ldots, 0.35, 0.40\}$ and the hole sides were calculated based on R as $d = \sqrt{Rp^2}$. The perforation pitch p is fixed for all cases as 16 μm.

In total, 9 different geometries were considered; the chosen values are shown in Table 2. The colors in the table represent the cases throughout all the figures in the paper. For the analytical approximation, only the means over modes are considered, shown in Figure 4.

4.1. Results

In the spirit of enhancing interpretability, it is desirable to find an analytical approximation in a form that allows us later to obtain the effective Young modulus E^* and effective plate density ρ^*.

Therefore, it was opted for rational functions instead of, e.g. quadratic polynomials, that would provide a fit of equal quality in terms of errors. So, the approximate formulation of the normalized frequency can be then

Case	1	2	3	4	5	6	7	8	9
a (μm)	72	96	120	144	168	192	72	96	120
h (μm)	1.125	1.500	1.875	2.250	2.625	3.000	2.250	3.000	3.750
$2a/h$	128	128	128	128	128	128	64	64	64
$N = (2a/p) \times (2a/p)$	9×9	12×12	15×15	18×18	21×21	24×24	9×9	12×12	15×15

Table 2: Plate dimensions. The colors represent the cases throughout all the figures in the paper.

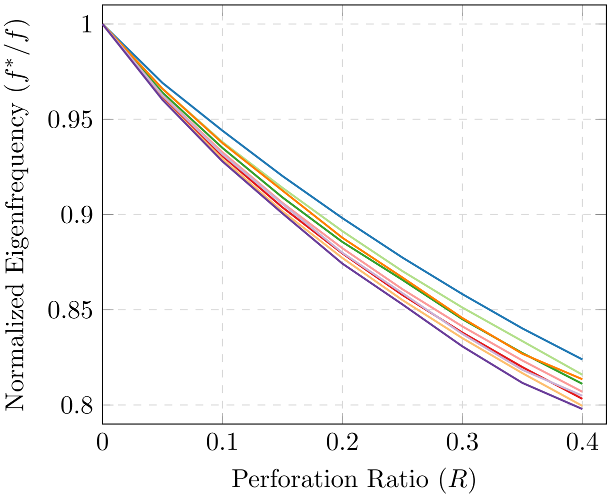

Figure 4: Normalized eigenfrequency, mean of the first eight modes for all cases 1 to 9.

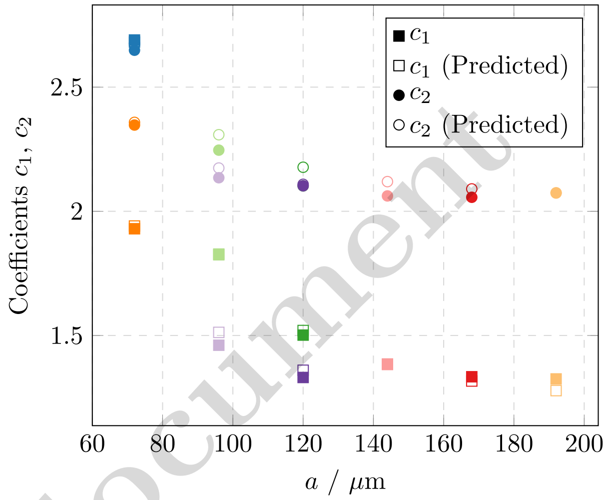

Figure 5: Coefficients c_1 and c_2. Full markers represent the calculated values based on COMSOL simulation, empty markers the values predicted by Eqs. (10)-(11).

written in the form

$$f^*/f = \frac{g_1(R)}{g_2(R)} = \frac{\alpha_1 R + \alpha_2}{\alpha_3 R + \alpha_4} \ , \tag{8}$$

where α_i are coefficients of the rational fit.
It turned out that only two parameters for the rational function are enough so that

$$f^*/f = \frac{R + c_1}{c_2 R + c_1} \tag{9}$$

where c_1, c_2 are dimensionless coefficients that depend on the plate geometry (see their values in Figure 5). Using least squares method (`curve_fit` from `scikit.optimize`), we identify the numerical values of c_1, c_2 from fitting the curves in Eq. Figure 4 with (9). The values of c_1, c_2 are different for each geometry, see full markers in Figure 5.
To find analytical approximation of c_1, c_2, these parameters were subsequently fitted using symbolic regression, searching over the space with operators `+,-,*,/,^`. The independent variables involved in the search were a, h, p together with plate surface a^2 and plate volume $V = a^2 h$.
Following Ockham's razor principle, it can be assumed that the resulting model should be sparse and not overly complicated. An approximation that shows reasonable tradeoff between sparsity and accuracy, reads

$$c_1 = 1.20 + \frac{8.64 V_{\text{norm}}}{V} \ , \tag{10}$$

$$c_2 = 2.04 + \frac{3.71 V_{\text{norm}}}{V} \ , \tag{11}$$

where V_{norm} is a volume chosen to make the coefficients dimensionless, $V_{\text{norm}} = 10\ \mu m \times 10\ \mu m \times 1\ \mu m = 10^{-16}\ \text{m}^3$.

Note that the coefficients could depend on the number of holes $N = (2a/p)^2$ times the thickness h, instead of the volume. Whether it is so, remains an unresolved case for the chosen dataset, as all of the cases in our dataset share the same pitch p, and should be investigated in the future.

The predicted normalized eigenfrequency matches the expected results very closely, as can be seen in Figure 6.

The expression for the effective eigenfrequency then reads

$$f^* = \frac{R + c_1}{c_2 R + c_1} f \ . \tag{12}$$

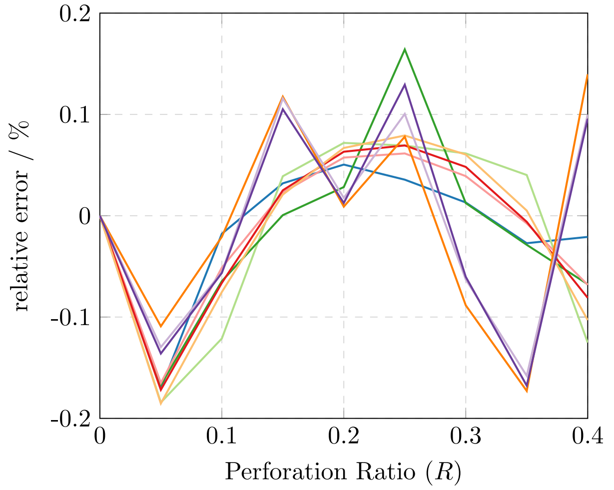

Figure 6: Relative error of the normalized eigenfrequency prediction.

Substituting Eq. (5) for f gives

$$f^*_{mn} = \frac{R+c_1}{c_2R+c_1}\frac{0.201}{a^2}\sqrt{\frac{(m+n)^{5.6}}{(mn)^{1.16}}}\sqrt{\frac{Eh^2}{12(1-\nu^2)\rho}} \tag{13}$$

$$= \sqrt{\frac{E(R+c_1)^2}{\rho(c_2R+c_1)^2}}\frac{0.201}{a^2}\sqrt{\frac{(m+n)^{5.6}}{(mn)^{1.16}}}\sqrt{\frac{1}{12(1-\nu^2)}} \; . \tag{14}$$

Assuming constant Poisson ratio, we can derive from this expression the effective Young's modulus E^* and the effective density ρ^*. With increasing perforation size d (i.e. increasing R), the effective Young's modulus E^* and effective plate density ρ^* are expected to decrease. The normalized effective Young's modulus E^*/E and normalized effective plate density ρ^*/ρ need to be equal to 1 for non-perforated plates (i.e., when $R = 0$).

With respect to these requirements, the corresponding form of the effective Young's modulus can be denoted as

$$E^* = E\frac{c_1^2}{(c_2R+c_1)^2} \; , \tag{15}$$

and the effective density as

$$\rho^* = \rho\frac{c_1^2}{(R+c_1)^2} \; . \tag{16}$$

5. Conclusion

For plates with all edges clamped, there are no known exact analytical solutions that satisfy the governing equation and boundary conditions. In this work, we provide analytical approximations for the eigenfrequencies of non-perforated and perforated square plates. The analytical approximation for the perforated plates is provided as a discrepancy to the solid plate and it is chosen in the form of a rational function characterized by only two geometry-dependent parameters. This choice allows for the subsequent derivation of the effective Young's modulus E^* and the effective plate density ρ^*.

6. Acknowledgments

A.F. acknowledges support by the Grant Agency of the Czech Technical University in Prague, grant No. SGS25/136/OHK3/3T/13.

References

[1] P. Malcovati and A. Baschirotto, "The evolution of integrated interfaces for mems microphones," *Micromachines*, vol. 9, no. 7, 2018, ISSN: 2072-666X. DOI: 10.3390/mi9070323.

[2] A. Dehé, "Silicon microphone development and application," *Sensors and Actuators A: Physical*, vol. 133, no. 2, pp. 283–287, 2007, ISSN: 0924-4247. DOI: 10.1016/j.sna.2006.06.035.

[3] N. N. Peña-García, L. A. Aguilera-Cortés, M. A. González-Palacios, J.-P. Raskin, and A. L. Herrera-May, "Design and modeling of a mems dual-backplate capacitive microphone with spring-supported diaphragm for mobile device applications," *Sensors*, vol. 18, no. 10, 2018, ISSN: 1424-8220. DOI: 10.3390/s18103545.

[4] K. Šimonová and P. Honzík, "Modeling of MEMS Transducers with Perforated Moving Electrodes," *Micromachines*, vol. 14, no. 5, p. 921, Apr. 2023, ISSN: 2072-666X. DOI: 10.3390/mi14050921.

[5] P. Deepak, s. Gawade, and D. K. Mali, "Dynamic response analysis of rectangular perforated plates with varying sizes of circular perforation holes," vol. 1, Jan. 2007.

[6] G. Kronberger, B. Burlacu, M. Kommenda, S. M. Winkler, and M. Affenzeller, *Symbolic Regression*, 1st ed. Boca Raton: Chapman and Hall/CRC, Jul. 2024, ISBN: 978-1-315-16640-7. DOI: 10.1201/9781315166407.

[7] Y. Xing, G. Li, and Y. Yuan, "A review of the analytical solution methods for the eigenvalue problems of rectangular plates," *International Journal of Mechanical Sciences*, vol. 221, p. 107 171, May 2022, ISSN: 00207403. DOI: 10.1016/j.ijmecsci.2022.107171.

[8] A. W. Leissa, "Vibration of Plates," 1969.

[9] K. Šimonová, P. Honzík, M. Bruneau, and P. Gatignol, "Modelling approach for MEMS transducers with rectangular clamped plate loaded by a thin fluid layer," *Journal of Sound and Vibration*, vol. 473, p. 115 246, May 2020, ISSN: 0022460X. DOI: 10.1016/j.jsv.2020.115246.

[10] M. Cranmer, *Interpretable machine learning for science with pysr and symbolicregression.jl*, 2023. DOI: 10.48550/ARXIV.2305.01582.

[11] K. F. Graff, *Wave Motion in Elastic Solids*. 1975.

[12] M. J. Jhung and K. H. Jeong, "Free vibration analysis of perforated plate with square penetration pattern using equivalent material properties," *Nuclear Engineering and Technology*, vol. 47, no. 4, pp. 500–511, Jun. 2015, ISSN: 17385733. DOI: 10.1016/j.net.2015.01.012.